PNAS RESEARCH ARTICLE | ECOLOGY

Grow now, pay later: When should a bacterium go into debt?

Jaime G. Lopez[a,b,c], Yaïr Hein[d], and Amir Erez[b,1]

Edited by Alan Hastings, University of California, Davis, CA; received August 28, 2023; accepted March 3, 2024

Microbes grow in a wide variety of environments and must balance growth and stress resistance. Despite the prevalence of such trade-offs, understanding of their role in nonsteady environments is limited. In this study, we introduce a mathematical model of "growth debt," where microbes grow rapidly initially, paying later with slower growth or heightened mortality. We first compare our model to a classical chemostat experiment, validating our proposed dynamics and quantifying *Escherichia coli*'s stress resistance dynamics. Extending the chemostat theory to include serial-dilution cultures, we derive phase diagrams for the persistence of "debtor" microbes. We find that debtors cannot coexist with nondebtors if "payment" is increased mortality but can coexist if it lowers enzyme affinity. Surprisingly, weak noise considerably extends the persistence of resistance elements, pertinent for antibiotic resistance management. Our microbial debt theory, broadly applicable across many environments, bridges the gap between chemostat and serial dilution systems.

microbial | consumer–resource | competition | antimicrobial

Significance

Microbes live in an uncertain world: A nutrient-rich environment can rapidly turn hostile with changes in temperature or the entry of antimicrobial compounds. There is an intrinsic trade-off between preparing for such stressors and capitalizing on immediate growth. How microbes approach this trade-off is of substantial practical concern, determining the spread of antimicrobial resistance (AMR). Here, we develop a mathematical theory to understand how microbes manage these trade-offs in time-varying environments. Our framework provides simple, experimentally accessible predictions on when these growth trade-offs become ecologically advantageous in different environments. Importantly, the theory predicts that even small noise in stressor concentration can massively extend the ecological lifetime of resistance elements, with implications for AMR management.

Microorganisms have shaped the world we live in and have adapted to thrive almost anywhere, including the human body, desert soils, forest soils, and coral reefs (1–4). Competition for limited resources is a central characteristic of microbial life, and this fierce competition, ongoing since the first cell emerged billions of years ago, has led microbes to explore astonishing ways to gain a growth advantage. However, our understanding of the core principles behind microbial competition remains mostly limited to steady environments.

In the microbial world, organisms commonly make a trade-off between hedging against future adverse events and maximizing immediate growth (5). This trade-off manifests in a variety of ecological contexts, many of them relevant to human health. For example, carrying the genes necessary to resist antibiotics slows a microorganism's growth in the absence of antibiotic, but the organism's growth will be maintained if antibiotics enter the environment (6–9). Similarly, the malaria parasite *Plasmodium falciparum* incurs a substantial growth defect by carrying a mutation that protects from antimalarial drugs (10). This trade-off is not limited to drug resistance: Mutations in regulatory elements, such as *Escherichia coli*'s *rpoS*, allow organisms to trade-off nutritional competence and general stress resistance (11, 12). In principle, a similar tradeoff could be driven by nongenetic mechanisms as observed in antibiotic persistence (13–16). To understand the core principle behind this "grow now, pay later" phenomenon, we introduce the metaphor of microbial debt—in which lacking the response capacity to future adverse events, reaps an immediate speedup in growth that is then "paid back" in the future. So, debtors are species that shift cost to the future (similar to interest paid on a loan) to gain a benefit in the present. Yet, despite the ubiquity of debt-like mechanisms in nature, theoretical understanding of debt in nonsteady environments is missing.

Debt causes a shift of cost from the present to the future, and its effect is thereby strongly tied to temporal variation. Temporal variation is a known driver of ecoevolution, impacting systems ranging from the microbiota of the Hadza people of East Africa (17), the mucosa of mice (18), and antibiotic resistance evolution (19). Evolutionarily, temporal variation can reduce the efficiency of natural selection and increase the fixation probability of mutations (20). Perhaps the simplest, yet most experimentally prevalent, example of temporal variation is serial-dilution batch culture—in which microbes are subject to periodic dilution and nutrient replenishment. This is substantially different from the chemostats—another common experimental system in which nutrient supply and dilution occur continuously (21). Studying and comparing the behaviors of chemostat and serial dilution systems, which represent two extremes of environmental variation, can provide insights into the environmental fluctuations present in real ecosystems. Although serial-dilution culturing is ubiquitous in experimental work (22, 23), modeling efforts in this direction are still incomplete (24–27). In the context of serial dilution cultures, we have recently shown that the effect of temporal variation

Author contributions: J.G.L. and A.E. designed research; J.G.L., Y.H., and A.E. performed research; J.G.L., Y.H., and A.E. analyzed data; and J.G.L. and A.E. wrote the paper.

The authors declare no competing interest.

This article is a PNAS Direct Submission.

[1]To whom correspondence may be addressed. Email: amir.erez1@mail.huji.ac.il.

This article contains supporting information online at https://www.pnas.org/lookup/suppl/doi:10.1073/pnas.2314900121/-/DCSupplemental.

Published April 8, 2024.

can be understood through the "early-bird" effect (24). The early-bird effect arises from the temporal gap between the introduction of nutrients and the inoculating mixture of microbes (at $t = 0$, simultaneously); and the transfer of a fraction of the culture to inoculate the next batch (a dilution event, at $t = t_f$). During this time, the early-bird species exhibit rapid growth at the onset of the batch cycle. Although their per-capita growth diminishes later in the batch cycle, the significant size of the "early-bird" species can still consume nutrients, consequently inhibiting the growth of "late-bird" species. This effect can cause shifts in community structure, shifts that do not occur in an equivalent chemostat. The early-bird effect has recently been shown to control the assembly of gut microbiome-derived ex vivo communities (28). It suggests a possible advantage, unique to serial-dilution cultures: to pursue a "debt" or "grow now, pay later" strategy which accelerates early growth by shifting costs to the future.

Much theory has focused on the dynamics of microbial debt trade-offs in fixed, chemostat-like conditions, showing that debt trade-offs can enable coexistence of strains (29, 30). In some cases, predictions from these chemostat theories have been qualitatively verified experimentally (31). While these trade-offs have been explored extensively in steady environments, less is understood about their dynamics in fluctuating environments. Contemporary understanding of the ecology of antibiotic resistance suggests that variation can substantially alter the value of debt (32), consistent with prior ecological theory on temporal variation (33) and highlighting the need for further work. Biophysical theories have been developed that predict optimal growth behaviors of microbes under environmental fluctuations, frameworks which can be applied to stress resistance phenotypes (14, 34). However, despite recent progress (35), there remains a pressing need for a comprehensive theoretical framework for trade-offs in serial dilution systems, bridging across commonly used experimental setups.

In this manuscript we ask: What are the consequences of accruing debt for a microbe within the context of a consumer–resource model? How does debt impact the growth dynamics of microbial communities under serial-dilution conditions compared to those in chemostat environments? We develop a modeling framework to explore microbial debt and demonstrate its use to analyze previously published experimental data. Our theory makes no assumptions about the shape of the debt trade-off surface (9, 31, 36). Though we consider only fixed and unchanging trade-offs, it is possible to extend the model to account for non-genetic adaptation (37). Our proposed model mimics a typical serial-dilution experimental procedure, while also being directly applicable to chemostats. We study the competition between two species, a debtor and a nondebtor, and find that when debt is compensated for by increased mortality, coexistence cannot occur between debtor and nondebtor, regardless of whether the mortality occurs in a punctuated or continuous manner. However, when debt is paid through decreased metabolic enzyme affinity, a stable coexistence state emerges. Intriguingly, when the cost of debt is subject to noise, the losing species can survive for a much longer time when compared to an equivalent deterministic system. Therefore, noise can enhance the persistence of antibiotic resistance elements.

Results

Chemostat Dynamics Reveal Growth-Debt Regulation in *E. coli*. Before introducing our serial dilution model, we first present the equivalent chemostat model as a baseline for the serial dilution results and as a bridge to the existing, chemostat-dominated literature. A single nutrient is provided at flux S, and its concentration within the chemostat is denoted $c(t)$. The chemostat is well mixed and constantly diluted with dilution rate δ. Let Species N be a nondebtor (a microbe with resistance to the stressor) with biomass density $\rho_N(t)$. Nutrient uptake is controlled by $g[c(t)]$, and growth is proportional to nutrient uptake. The per-capita growth rate of Species N is $E\,g[c(t)]$ where E defines the maximal per-capita growth rate. In contrast, Species D, the debtor species, with biomass density $\rho_D(t)$, has a higher maximal growth rate, $E+\Delta E$ due to sacrificing its stress resistance capability and diverting these resources to immediate growth. The lack of stress resistance leads to constant stress-induced death at rate ω. The equations governing these chemostat dynamics are therefore: $\frac{1}{\rho_N}\frac{d\rho_N}{dt} = Eg[c]-\delta$; $\frac{1}{\rho_D}\frac{d\rho_D}{dt} = (E+\Delta_E)g[c]-\delta-\omega$; and $\frac{dc}{dt} = S-\rho_D(E+\Delta_E)g[c]-\rho_N Eg[c]$. We show this model is equivalent to a more general chemostat model with more variable growth parameters in *SI Appendix*, 2. Note that we neglect δc in the nutrient dynamics as the dominant nutrient depletion term comes from the bacterial consumption (29, 38).

To validate our model assumptions and quantitatively show the existence of debt trade-offs, we apply this chemostat model to the classical experiments of Notley-McRobb et al. (11). These experiments studied competition between wild-type (WT) *E. coli* and mutants with defective *rpoS* genes, the transcription factor governing stress response in *E. coli*. Here, the WT plays the role of nondebtor and the mutants are debtors. In Fig. 1*A*, we show the relative abundance of the nondebtor WT strain in chemostats operating at different dilution rates. In these low-stress chemostats, the community is rapidly overtaken by the debtor *rpoS* mutants, well captured by our model fit (see *SI Appendix*, 4 for details on fitting approach and methods). However, these debtors have traded growth rate against stress resistance, and are now far more vulnerable to stress. In Fig. 1*B*, we show the temperature stress response of the community from one chemostat as the debtor population increases. Initially, the population is composed of nondebtors and many bacteria survive the stressor. However, once debtors sweep the population almost no bacteria survive the stressor. These stress survival dynamics are well described by our model fit. Thus, debt trade-offs occur within *E. coli* and are quantitatively consistent with our model assumptions

In this chemostat formalism, when is growth debt worthwhile? For this calculation, we define $g[c]$ as the classical Monod function $\frac{c}{c+K}$, where K is the half-saturation coefficient. By comparing the competitive ability of the nondebtor and debtor, we determine that a stressor death penalty ω is worthwhile if the corresponding benefit Δ_E satisfies:

$$\omega/\delta \leq \Delta_E/E, \qquad [1]$$

(For details, see *SI Appendix*, 1). Thus, at a higher dilution rate, δ, the relative cost of debt decreases. Eq. **1** predicts that at perfect equilibrium, a linear relationship exists between the inverse dilution rate $1/\delta$ and the growth advantage Δ_E/E. Therefore, to be consistent with the debtor mutants taking over the population, as observed by Notley-McRobb (11), the cost of debt should be smaller than this upper limit. In Fig. 1*C*, we show the growth advantage of debtor mutants as a function of inverse dilution rate. The debtor mutant Δ_E/E is a reflection of *E. coli*'s investment in stress resistance. A large debtor advantage indicates that the nondebtor invests more resources in stress response, while a small advantage indicates little investment. The linear relationship shown in Fig. 1*C* indicates *E. coli* invests less in stress resistance at higher growth rates: when $1/\delta$ is small, for the debtor to take over, a smaller Δ_E/E is required, in a proportional manner consistent with our theory.

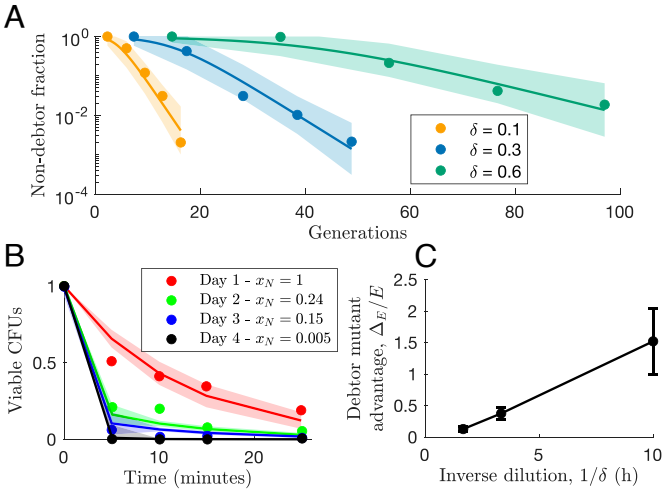

Fig. 1. Application of chemostat theory to experiments of Notley-McRobb et al. validates model assumptions and shows existence of trade-offs between maximal growth rate and stress resistance in *E. coli* (11). (*A*) Fit of chemostat theory to *rpoS* evolution trajectories in pH 7 glucose-limited chemostats at three different dilution rates δ. Fit parameters: $\Delta_E/E = [1.52 \pm 0.52, 0.37 \pm 0.1, 0.13 \pm 0.04]$ at $\delta = [0.1, 0.3, 0.6]$ h^{-1}, respectively, and 0.025 ± 0.05. (*B*) Fit of theory to community temperature stress assay at 60 °C. Samples taken from glucose-limited $\delta = 0.3$ h^{-1} chemostats at different days. Fit parameters: $\omega_N = 0.084 \pm 0.014$ min^{-1} and $\omega_D = 0.99 \pm 1.92$ min^{-1}. (*C*) Plot of debtor mutant advantage Δ_E/E as a function of inverse dilution rate $1/\delta$. Values from fit in *A*.

Similar chemostat theories to those presented here have been further developed. For example, it has been shown that with additional information about the form of the *rpoS* trade-off surface, one can qualitatively predict the outcome of *E. coli* evolution within a chemostat (31). However, what happens away from chemostat conditions in a fluctuating serial dilution environment?

Serial Dilution Model Formulation. We now establish our serial dilution model where two species compete for a single, limiting nutrient in an environment influenced by a stressor. In a serial dilution culture, microbes are grown in a well-mixed environment for a given period of time, t_f, before being diluted into fresh media and allowed to grow again. We refer to the new nutrient added after dilution as the "nutrient bolus." A single type of nutrient is provided, and its concentration within a batch is denoted $c(t)$ with $c(t=0) = c_0$. As in the chemostat, let Species N be a nondebtor (a microbe with resistance to the stressor) with biomass density $\rho_N(t)$, with per-capita growth rate $E\,g[c]$. In contrast, Species D, the debtor species, with biomass density $\rho_D(t)$, has higher maximal growth rate, $E + \Delta_E$ due to sacrificing its stress resistance capability. The lack of stress resistance leads to two possible forms of stress-induced death: a continuous death rate per unit time (ω), and/or, an increased dilution during dilution events (Ω). The within-batch dynamics are therefore:

$$\begin{aligned}
\frac{dc}{dt} &= -g[c]\left(E\,\rho_N + (E+\Delta_E)\,\rho_D\right), \\
\frac{1}{\rho_N}\frac{d\rho_N}{dt} &= E\,g[c] - \omega_N, \\
\frac{1}{\rho_D}\frac{d\rho_D}{dt} &= (E+\Delta_E)\,g[c] - \omega_D. \qquad [2]
\end{aligned}$$

Here, ω_N and ω_D are the nondebtor and debtor within-batch death rates, respectively. These death rates could be the result of an antibiotic in the media or another stressor, such as temperature, salinity, or pH. Note that the terms on the right-hand side of the equations for $\rho_{N/D}$ are the per-capita growth rates. It is possible to render these equations dimensionless by measuring time in units of E, and concentration in units of K (cf. *SI Appendix*, 5). However, since our model is easily applicable to experimental data, we keep the dimensionful version of these dynamics for more direct data comparison.

The second source of mortality in the model is not continuous, but rather punctuated, happening only at the transition between batches. We refer to the transition from batch to batch as "dilution," reflecting what occurs in laboratory serial dilution, but it represents any number of potential punctuated stressors, such as sudden heat or osmotic shock. When dilution happens, each species is diluted by its species-specific factor Ω_N or Ω_D. Thereby, dilution in our model generalizes the typical scenario where a small volume of a well-mixed culture is used to inoculate the next batch, diluting each species equally. In this generalized version, the total inoculum size, $\rho_N(0) + \rho_D(0)$, can vary from batch to batch until steady state is reached. A schematic of these mechanisms is shown in Fig. 2*A*. At the end time (t_f) of batch b, each species gets diluted differently, and so, at the beginning of batch $b+1$,

$$\begin{aligned}
\rho_N^{(b+1)}(t=0) &= e^{-\Omega_N t_f}\left(\frac{\rho_0}{\rho_0 + c_0}\right)\rho_N^{(b)}(t_f), \\
\rho_D^{(b+1)}(t=0) &= e^{-\Omega_D t_f}\left(\frac{\rho_0}{\rho_0 + c_0}\right)\rho_D^{(b)}(t_f). \qquad [3]
\end{aligned}$$

In the rest of this manuscript, we set $\Omega_N = \omega_N = 0$ and drop the subscript from Ω_D and ω_D.

Nutrient utilization, g[c(t)]. We considered two general forms of the utilization function $g[c]$: utilization that is proportional to the

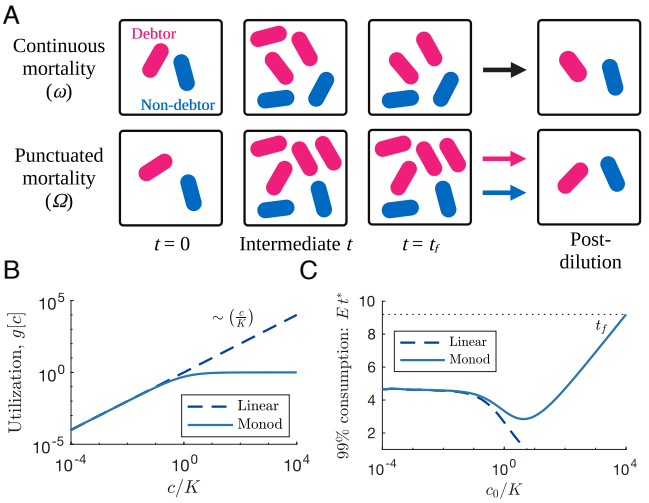

Fig. 2. Overview of serial dilution ecosystem with debt. (*A*) Schematic of the serial dilution system with debt. In the continuous death case, the debtor is able to initially grow more quickly, but loses biomass continuously. In the punctuated death case, the debtor grows more quickly but is diluted more severely at the end of the batch. (*B*) Example of growth functions. Linear is $g[c] = Ec$, and Monod is $g[c] = E\left(\frac{c}{c+K}\right)$. (*C*) Time necessary for a single nondebtor species to deplete 99% of the supplied nutrient t^* for different growth functions. In order to choose a single t_f that is sufficiently long, we select the t^* for $c_0/K = 10^4$ with a Monod growth function.

nutrient concentration, $c(t)$, and utilization that obeys Monod-like nonlinearity. Specifically,

$$g[c] = \begin{cases} \frac{c}{c+K} & \text{Monod} \\ \frac{c}{K} & \text{Linear} \end{cases} \quad [4]$$

The Monod function (21) when $c \ll K$ corresponds to linear consumption. At the opposite limit, at high nutrient concentration, linear consumption is nonphysical as it implies that a huge quantity of nutrient would be consumed almost instantly. The Monod case is well established to model microbial nutrient utilization (Fig. 2*B*). A generalization of the Monod form is considered in *SI Appendix*, 8. For the rest of this manuscript, we thus focus on the Monod form.

Batch time, t_f. When modeling serial dilution, it is possible to choose the batch time t_f to be as long as necessary to consume all resources (24, 25). However, here we also considered within-batch mortality, and therefore arbitrarily long batches would lead to the extinction of the susceptible species. A more realistic view, in line with experimental practices, sets a fixed batch time, t_f. The time needed for consumption of most of the nutrient depends on how much nutrient is provided. In this study, we varied the supplied nutrient concentration, c_0, over six orders of magnitude. To ensure that most of the nutrient is consumed in all relevant scenarios, we define t_f based on the nutrient utilization at high c_0. Assuming Monod utilization with only one species present, t_f is defined as the time it takes to consume 99% of c_0 with $c_0/K = 10^4$. Thereby, we ensure that at least 99% of the nutrient will be consumed for all relevant scenarios explored in this work. The dependence of t_f on c_0, while maintaining $\frac{c_0 - c(t_f)}{c_0} = 0.99$, is shown in Fig. 2*C*.

Equivalent Value of Debt Represented as Continuous and Punctuated Mortality. In our model, when is microbial debt worthwhile? Does it matter if the debt incurred is paid for in a continuous or punctuated fashion? We quantify debt by considering the dynamics within a single batch, i.e., a single growth and dilution cycle. At a given batch b, it is possible to integrate Eq. **2**, given the initial inocula concentrations $\rho^{(b)}_{N,D}(0)$. At the end of this batch, $t = t_f$, we have the following populations:

$$\begin{aligned} \rho^{(b)}_N(t_f) &= \rho^{(b)}_N(0) e^{E\int_0^{t_f} g[c(t')]\,dt'}, \\ \rho^{(b)}_D(t_f) &= \rho^{(b)}_D(0) e^{E(1+\frac{\Delta_E}{E})\int_0^{t_f} g[c(t')]\,dt' - \omega t_f}. \end{aligned} \quad [5]$$

When going to the next batch, the debtor species gets diluted by a multiplicative factor $e^{-\Omega t_f}$ beyond the $\frac{\rho_0}{\rho_0+c_0}$ factor both species get diluted by. Therefore, at the beginning of batch $b+1$,

$$\begin{aligned} \rho^{(b+1)}_N(0) &= \frac{\rho_0}{\rho_0 + c_0}\,\rho^{(b)}_N(t_f), \\ \rho^{(b+1)}_D(0) &= e^{-\Omega t_f}\frac{\rho_0}{\rho_0 + c_0}\,\rho^{(b)}_D(t_f). \end{aligned} \quad [6]$$

At steady state, equal growth implies that both species are increased and decreased by the same fold-change. Therefore, coexistence implies that,

$$\underbrace{\left(\frac{1}{t_f}\int_0^{t_f} g[c(t')]\,dt'\right)}_{\text{Time-averaged nutrient utilization}} \underbrace{\Delta_E}_{\text{Benefit per utilization}} = \underbrace{\omega + \Omega}_{\text{Cost}}. \quad [7]$$

Eq. **7** states that coexistence balances growth cost with benefit: the growth benefit per nutrient utilized times the time-averaged nutrient utilization equals the cost. In essence, the benefit from accruing the debt in the form of increased growth must be equal to the death cost incurred. This expression defines the border between regimes in which debt is favorable and those in which it is unfavorable Fig. 3*A*. In this choice of parametrization, the two forms of debt, continuous (ω) and punctuated (Ω), are equivalent and their rates are additive.

Importantly, in the single-species case, even away from steady state, the nutrient utilization integral is independent of $g[c]$ if the vast majority of the nutrients are consumed within the batch, with $\int_0^{t_f} g[c(t)]\,dt \approx \frac{1}{E}\log\left(1+\frac{c_0}{\rho_0}\right)$ by mass balance. Note that $1+\frac{c_0}{\rho_0}$ is the dilution factor of the serial dilution system, a property determined by the experimentalist. This is a tremendous simplification, since knowledge of $g[c]$ is unnecessary. It is especially useful to parameterize experimental monoculture dynamics, without having to measure $g[c]$. For example, application to an antibiotic resistance measurement requires only the element's carriage cost and the death rate of cells without the resistance elements.

What happens when the debtor and nondebtor have different nutrient-to-biomass conversion coefficients (yield)? We may modify Eq. **5** to include yields by taking $E \to Y_N E$ and $(E+\Delta_E) \to Y_D(E+\Delta_E)$. Then the cost–benefit balance, Eq. **7**, becomes $\left(\frac{1}{t_f}\int_0^{t_f} g[c(t')]\,dt'\right)\left[\Delta_E + E\left(1-\frac{Y_N}{Y_D}\right)\right] = \frac{\omega}{Y_D}$. Therefore: i) the time-averaged nutrient utilization term, $\frac{1}{t_f}\int g\,dt'$, remains the same; ii) The debtor's yield, Y_D, rescales the cost of debt so that larger debtor yield allows larger debt; iii) Interestingly, there is a contribution that is independent of the debtor benefit per utilization, Δ_E. Instead, it stems from a difference between the nondebtor and debtor yields. Accordingly, the debtor may remain competitive while incurring debt without a maximal-growth-rate benefit, if it achieves higher yield than the nondebtor. Thus, another debt-growth tradeoff exists: The debtor can offset the cost of decreased stress resistance by increasing yield.

We may similarly consider the chemostat limit of the serial-dilution dynamics with yield. By substituting $\omega \to \frac{\omega}{Y_D}$ and $\frac{\Delta_E}{E} \to \frac{\Delta_E}{E} + \left(1-\frac{Y_N}{Y_D}\right)$ we attain the chemostat coexistence

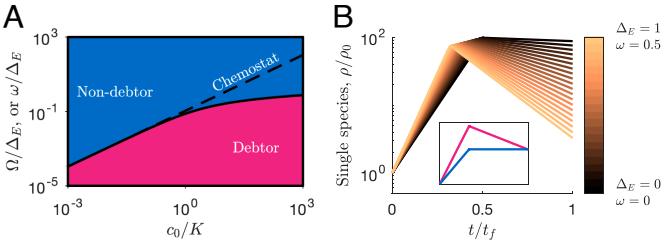

Fig. 3. Serial dilution results in (*A*) Phase diagram of competition between debtor and nondebtor as a function of bolus size c_0/K and normalized death penalty. The dashed line represents the phase boundary for the equivalent chemostat system, diverging substantially from the serial dilution phase boundary at high c_0/K. This phase diagram captures both continuous and punctuated death, with the *y*-axis being equivalently Ω/Δ_E or ω/Δ_E (*B*) Within-batch dynamics of a single species along the $\Delta E, \omega$ trade-off. Note that while the debtor species grows rapidly initially, its final biomass may be much lower due to death. *Inset*: (same axes). In competition with a nondebtor, the increased early growth of the debtor consumes the nutrient and denies nutrient from the nondebtor.

condition that was derived directly from the chemostat version of the dynamics in *SI Appendix*, 2. Thus, the same rescaling of the cost with Y_D and the growth gain from the difference in yields applies in the chemostat limit of the serial-dilution dynamics.

Serial Dilution Cultures Show Diminishing Return on Debt at High Nutrient Concentrations When Compared to a Chemostat. We have determined the phase diagram for debt favorability in a serial dilution system, but how does this compare to a system with continuously supplied nutrient, i.e., a chemostat? If we add a very small bolus, $c_0 \ll K$, then dilute the culture by a fraction close to 1, and repeat, it stands to reason that the limiting behavior becomes continuous in time. As $c_0/K \to 0$, the serial dilutions become effectively a chemostat, and so, we expect that the continuous and punctuated dilution cases have the same chemostat limit. To consider $c_0 \ll K$, the chemostat limit, we follow ref. 24, and linearize the dynamics around the small parameter c_0/K (for details see *SI Appendix*, 6). The chemostat cost–benefit tradeoff then becomes $\frac{\Omega+\omega}{\Delta_E} \approx \frac{c_0}{\rho_0 E t_f}$, shown as the dashed line in Fig. 3*A*. It is satisfying to note that this is equivalent to the linear chemostat debt relation in Eq. **1** and thus also consistent with the experimental analysis shown in Fig. 1*C*.

Why does the boundary between debtor and nondebtor dominance in the serial-dilution culture deviate from its equivalent chemostat at large c_0? There is a diminishing return on debt as more nutrient is supplied. The diminishing return and its relation to the early-bird effect can be understood from Fig. 3*B*, showing time-series of a debtor in a single batch, grown in monoculture, with several values of (ω, Δ_E) pairs. The pairs lie along the coexistence boundary with the nondebtor (Fig. 3*A*). As ω, Δ_E are increased, the species grow more rapidly initially, (higher slope in the semilog plot), then followed by an exponential loss because of ω (downward slope). The initial debt, which gives the rapid rise, is offset by the incurred death later in the batch. Indeed, when the nondebtor species is introduced in a coculture, both species reach the same level at the end of the batch (*Inset* of Fig. 3*B*). This demonstrates the early-bird effect since the debtor deprives the nondebtor from nutrient in the early growth phase, though finally the debtor settles at a much lower population size because of the debt payoff.

The results we have derived for both chemostat and serial dilution rely on the assumption that there is instantaneous use of the nutrient imported into cells for growth, but in reality there is time delay between import of nutrient and utilization of that nutrient for growth. In some types of cells with dedicated nutrient storage capacity, such as phosphate-accumulating organisms (39), this delay can be quite significant and potentially complicate debt dynamics. In *SI Appendix*, 3, we explore such time-delayed models. We find that these delays have little effect on our chemostat results, as the time delay has no impact on steady states when nutrients are supplied continuously. In the chemostat case, the time delay can be captured by an effective nondelayed growth function. Interestingly, trade-offs between nutrient import rate and internal growth rate due to internal nutrient amount manifest in this effective growth function similarly to trade-offs between maximum growth and nutrient affinity—explored in the following section. In the serial dilution case, the effect of the time delay depends on whether the internal nutrient pools are able to reach a pseudosteady state with respect to the external nutrient environment during the batch. If such a pseudosteady state is reached, the model outcome is similar to the model with no time delay, but now using the effective growth function instead of a Monod function. Using prior literature data from *E. coli* (*SI Appendix*, 3), we estimate that typical microbial growth operates in this regime. However, it is a different scenario if this pseudosteady state is not reached, e.g., if uptake of all nutrient within the environment occurs before appreciable growth occurs. In this fast-uptake scenario, the debt trade-off becomes entirely independent of the cell's internal growth parameters, instead being entirely controlled by the rate of nutrient import. Interestingly, the resulting phase diagram for nondebtor vs. debtor competition (*SI Appendix*, Fig. S2) is qualitatively similar to Fig. 3*A*. The role of the debtor cost, Ω/Δ_E, is taken by the inverse of the advantage in import rate. Thus, we find that our debt trade-off results are also applicable when allowing for nutrient import and storage.

Debts Involving a Growth Affinity Trade-Off Allow Coexistence. Thus far, we have examined trade-offs where the maximum growth rate under normal conditions is counterbalanced by mortality in the presence of a microbicidal stressor. However, there are other forms of growth stress and payment, e.g., there exist microbiostatic stressors that do not kill but rather inhibit the growth of microbes. The inhibition can be considered as a penalty on the maximum growth rate. Similarly, resistance mechanisms can affect growth properties other than the maximum growth rate. For example, resistance mutations may lead to a growth defect that manifests most strongly at low nutrient concentrations. Interestingly, the resistant phenotype (with higher maximal growth rate and lower enzyme affinity) is now playing the role of the debtor in a bacteriostatic environment, because it "grows now, pays later." The debtor in the bacteriostatic environment mutates its enzymes to avoid the bacteriostatic effect, thereby sacrificing its future growth at low nutrient concentration because the mutated enzymes have lower affinity.

In our framework, growth penalties that are most severe in low nutrient conditions would manifest in the Monod affinity, K, increasing to $K + \Delta_K$ (32, 40). Recent research on OmpF porin channels empirically demonstrates this trade-off: Mutants with enlarged pore sizes exhibit growth advantages in the absence of antimicrobial agents, by facilitating nutrient uptake. Yet the enlarged pores also increased antimicrobial entry into the cell. Conversely, mutants with narrower channels restrict antimicrobial entry but incur a growth cost, especially under low-nutrient conditions (9). We derive mechanistically how alterations in the efficiency of a transporter will manifest as an effective increase in K in *SI Appendix*, 3. This trade-off is most evident in serial-dilution cultures (9). Therefore, we shift our perspective and study the debt trade-off in which the debtor species has mutated so that it pays a growth cost in low-nutrient environment, but gains a maximal growth rate ΔE. How does this trade-off impact the value of debt?

We deduce the affinity-growth trade-off using an invasibility calculation: When would a minuscule amount of an "invader" species succeed in expanding under nutrient dynamics dictated by a single dominant nondebtor? Namely, a species with lower enzyme affinity, $K + \Delta_K$, but also higher maximal growth rate, $E + \Delta_E$, is introduced to a system dominated by the single-species dynamics of an unperturbed (K, E) species. How large does Δ_E need to be to offset the cost of the decreased affinity $K + \Delta_K$? Equivalent growth implies that $E\int_0^{t_f} \frac{c}{c+K}\,dt' = E\ln\left(1+\frac{c_0}{\rho_0}\right) = (E+\Delta_E)\int_0^{t_f} \frac{c}{c+K+\Delta_K}\,dt'$. Expanding the

perturbed Monod function at small Δ_K/K, with $f(K+\Delta_K) = f(K) + \left.\frac{df}{dK}\right|_K \Delta_K + O(\Delta_K^2)$, we write to leading order,

$$\underbrace{\int_0^{t_f} \frac{c\,dt'}{c+K+\Delta_K}}_{I(t_f)} = \underbrace{\int_0^{t_f} \frac{c\,dt'}{c+K}}_{I(t_f)} - \underbrace{\Delta_K \int_0^{t_f} \frac{c\,dt'}{(c+K)^2}}_{\Delta_I(t_f)}, \quad [8]$$

$$\frac{\Delta_E}{E} = \frac{\Delta_I}{I} = \Delta_K \frac{\int_0^{t_f} \frac{c}{(c+K)^2}\,dt'}{\int_0^{t_f} \frac{c}{c+K}\,dt'}.$$

At equilibrium, the relative gain in maximal growth rate, Δ_E/E, is offset by the relative loss in utilization, Δ_I/I. It is possible to approximate this relation at the low and high c_0 limits, (*SI Appendix*, 9). The integral Δ_I and its approximate forms are shown in Fig. 4*A*. To leading order, we have,

$$\frac{\Delta_E}{E} \approx \begin{cases} \frac{\Delta_K}{K} & c_0 \ll K \\ \frac{\Delta_K}{c_0}\left(1 + \frac{\ln(c_0/K)}{\ln(c_0/\rho_0)}\right) & c_0 \gg K \end{cases} \quad [9]$$

The relative cost at equilibrium behaves differently in the low c_0 (chemostat) and high c_0 limits. At low c_0, as in a chemostat, the cost scales with Δ_K. Therefore, for a given value of relative gain, Δ_E/E there is a fixed cost Δ_K/K to maintain equilibrium, no matter how much nutrient is provided. There is little enough nutrient provided such that the growth function is linear in the nutrient amount, leaving the difference in affinity, Δ_K, as the dominant term. A different picture emerges in the high c_0 limit, where nutrient is initially saturating. Here, for a fixed gain, Δ_E/E = const, the cost $\Delta_K \sim c_0$, meaning that to maintain equilibrium, if more nutrient is provided, a larger enzyme affinity penalty can be supported. Said differently, the debtor takes over for a fixed Δ_K if c_0 increases. The debtor advantage over the chemostat limit is shown in the horizontal tendency of the Δ_K/c_0 boundary in Fig. 4*B*. This is because 'payment' happens mostly when $c \approx K+\Delta_K$ and when $c_0 \gg K$ and Δ_K, a larger c_0 gives the debtor an increasing span of growth with effectively no payment.

To complete the invasibility test, one must consider the opposite situation, where the debtor dominates the culture, dictating the nutrient dynamics with $(K+\Delta_K, E+\Delta_E)$, and an invasion attempt by the nondebtor. When can the nondebtor invade? A similar derivation gives $\frac{\Delta_E}{E+\Delta_E} = \frac{\Delta_{I[K+\Delta_K]}}{I_{[K+\Delta_K]}}$, with the I and Δ_I integrals evolved under the debtor monoculture. As with the previous boundary, we may approximate, (*SI Appendix*, 9).

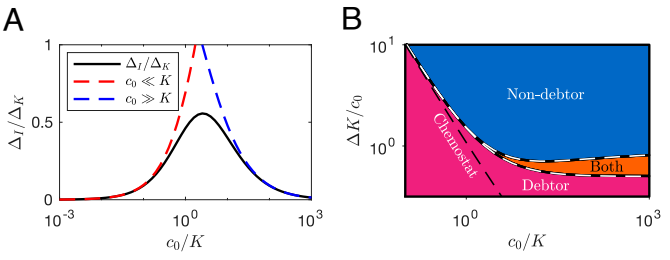

Fig. 4. The tradeoff between maximal growth rate, $E+\Delta_E$ and reduced affinity due to $K+\Delta_K$. (*A*) Δ_I/Δ_K depicts the loss of growth per biomass, and its low and high c_0/K approximations. (*B*) Phase diagram of the coexistence and dominance regimes, and its leading order analytic approximation (Eq. **9**, white dashes). Black dashes: The chemostat limit of the phase boundary. $E = \Delta_E = 1$ and $K = 1$. A coexistence region where both species support a nonzero population emerges high c_0.

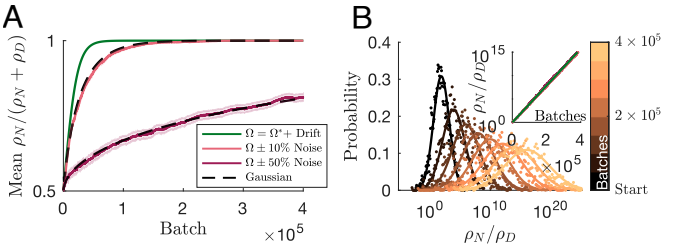

Fig. 5. The effect of noise in Ω. (*A*) Full curves—mean ρ_N fraction. Shaded area: SEM, averaged over 1,000 stochastic trajectories. Green curve—deterministic convergence to nondebtor take-over. Dashed black—Gaussian theory derived from the central limit theorem, cf. *SI Appendix*, 10. (*B*) Time-series of the distribution of $\log_{10}\rho_N/\rho_D$. Dots—distribution timeseries calculated numerically, from the first batch until 4×10^5 batches. The widening corresponds to a diffusion process and the drift to extinction of ρ_D. Curves—the corresponding Gaussian theory, cf. *SI Appendix*, 10. *Inset*: The constant drift in the median value of ρ_N/ρ_D, identical for all three noise levels, equivalent to the mode of the histograms.

Interestingly, a coexistence region emerges at high c_0/K (Fig. 4*B*). Coexistence is due to the different effect of the dominant species: Δ_E is measured against E when the nondebtor is dominant but against $E+\Delta_E$ when the debtor is dominant. This mode of coexistence is similar to that seen in another recent serial dilution theory (41) and falls into a broader class of "relative nonlinearity" coexistence mechanisms (33).

Stochastic Stressor Dynamics Significantly Lengthen Lifetime of Ecologically Unstable Species. The models explored in the prior sections exhibit temporal variability, but in a deterministic manner: dilution factors and stressor levels staying the same in all batch cycles. However, in real ecosystems, the magnitude of the stressor effect is variable. For example, antibiotic concentration fluctuates in the environment (19), leaving a debtor species disproportionately susceptible to extreme dilution. What is the effect of such stochastic noise on the debt cost–benefit tradeoff? Let Ω fluctuate, drawing Ω in each batch from a uniform distribution, $\Omega \in [\Omega-\Delta_\Omega, \Omega+\Delta_\Omega]$. This corresponds to "pink" or $1/\Omega$ noise where extreme events occur at very low probability.

We consider a system with $\Omega > \Omega^*$ such that the debtor is outcompeted in the deterministic version of the model. We show this deterministic trajectory, batch to batch, plotting the relative abundance of the nondebtor (Fig. 5*A*). To explore how this extinction process is affected by noise, we plot the stochastic trajectory averages of the equivalent system with two different levels of Ω noise. Alternatively, these results can be derived analytically using the central limit theorem, generalizing their applicability across a large class of noise distributions (cf. *SI Appendix*, 10). Intriguingly, the introduction of even a small level of noise, constituting 10% of Ω, significantly decelerates the extinction dynamics. With 10% noise, $\Omega \pm 10\%$, the time to extinction is approximately tripled, while with 50% noise, the time to extinction is lengthened by orders of magnitude (Fig. 5*A*). This behavior is symmetric to a reversal in roles: The same behavior occurs with nondebtor extinction if the environment favors debtors. Thus, noise in stressor severity can drastically extend the lifetime of ecologically unstable microbes.

How does this seemingly minor noise in Ω produce such drastic departures from the deterministic behavior? The key observation is that $\Omega\, t_f$ (and $\omega\, t_f$) act on the population abundances in logarithmic space (Eqs. **3** and **5**). Thus, rather than inducing a random walk of ρ_N in linear space (which would preserve the deterministic dynamics of the mean), this process is

instead a random walk in $\log(\rho_N/\rho_D)$. In Fig. 5*B* we plot the evolution of the distribution of the balance variable, $\log(\rho_N/\rho_D)$ (42). As can be seen, the balance undergoes a canonical biased random walk, with the distribution widening and simultaneously its mean drifting. The drift is due to the induced extinction because unfavorable debt conditions, $\Omega > \Omega^*$, were chosen. As expected, the mean $\log(\rho_N/\rho_D)$ of the different noise levels, including the deterministic dynamics, are all equal (Fig. 5 *B*, *Inset*). As is known, the balance or log-ratio is the appropriate degree of freedom to consider when studying the dynamics of a composition (43, 44). Indeed, balances would be the appropriate variables to consider in multispecies generalization of our framework. This random walk in logarithmic space has long tails for the relative abundances, $\frac{\rho_N}{\rho_N+\rho_D}$, a quantity typically relevant ecologically and measured in experiments. Thus, large, rare events significantly influence an observed mean fraction even when noise is relatively small. This suggests a broad distribution of stress resistance traits even within a single species, consistent with what has been observed in *E. coli* (12).

Conclusions and Discussion

Real-world microbes can incur debt by increasing immediate growth while neglecting protection from future events. Here, we proposed a theory for the impact of such debt trade-offs on microbial competition. We began by formulating chemostat debt dynamics and validating them with data from a classical chemostat experiment, thereby exposing the dynamic debt regulation behavior of *E. coli*. Notably, we validated the predicted linear relationship between the inverse dilution rate and the debtor advantage proposed by our chemostat theory. Having established the basic debt dynamics, we extended our theory to serial-dilution cultures. We found that growth debt where the "payment" occurs continuously and where it occurs at the end of the batch are equivalent and can be unified in a single framework. We then constructed a universal phase diagram that delineates the boundary where debt becomes competitively favorable, as a function of nutrient amount in the system. This phase diagram encompasses both serial dilution and chemostat dynamics, unifying the two experimental systems. In the chemostat, the trade-off line is proportional to the total nutrient supply. Conversely, in the serial dilution setup, the addition of nutrients in a saturating concentration results in a diminishing return on debt. The effect of diminished return can be considerable: a nondebtor that would typically go extinct in a high-nutrient chemostat may dominate an equivalent serial dilution culture. However, we found that not all forms of debt are the same: Debt associated with enzyme affinity allows the coexistence of two species on a single resource, violating the competitive exclusion principle by forming temporal niches (41).

Experiments to test the predicted phase boundaries would involve competitions between a debtor and nondebtor strain in varying serial dilution environments. One could monitor the persistence of an antibiotic resistance element in a community across a range of antibiotic and nutrient concentrations (thus varying ω and c_0/K) to construct an empirical version of the phase diagram in Fig. 3*A*. The debtor could be a WT *E. coli* with the nondebtor being that same strain with an antibiotic resistance element. Ideally, this element would confer resistance that does not inactivate the antibiotic (e.g., an efflux transporter), to prevent benefit to nonresistant organisms (45). The resulting phase diagram should feature a boundary defined by Eq. **7**. To construct a theoretical phase diagram for comparison, one could measure death kinetics as a function of antibiotic concentration, and in the absence of antibiotic use a competition experiment to infer the cost of the element. In the chemostat analysis (Fig. 1), we demonstrated how to estimate both values given a set of experimental data. Evolution may complicate such an experiment—discussed below.

Stochastic stressor dynamics, a realistic extension of the model, revealed unexpected behavior. Even small fluctuations in the stress level can significantly delay the extinction of a species due to the compositional nature of the serial-dilution process. To decouple the compositional effects, a log-ratio is used (42–44), here, $\log \frac{\rho_N}{\rho_D}$. As the system relaxes to steady state, the mean log-ratio dynamics are the same in the deterministic and stochastic systems. Conversely, the mean relative fraction $\frac{\rho_N}{\rho_N+\rho_D}$ changes greatly with the addition of noise, leading to delayed extinctions. The outcomes of our stochastic dynamics study hold considerable implications for the management and control of antibiotic resistance elements within environments. For example, rotating antibiotics to reduce the prevalence of resistance elements has been proposed as a means of limiting resistance proliferation (46). Our findings indicate that the timescale for the depletion of resistance elements in the environment may be significantly longer than deterministic models (47) would estimate, limiting the efficacy of rotation-based strategies. Our findings also extend beyond antibiotic resistance, implying that stress resistance genes could persist within communities for extended periods despite a net loss of fitness. Noisy debt dynamics may broadly influence the prevalence of accessory genes in bacteria.

The predictions on the influence of stressor noise on the lifespan of resistance elements can be experimentally tested. The model predicts that across many independent populations of cells, populations subject to a more noisy stressor are expected to have longer mean persistence of resistance elements (Fig. 5). One approach is to first identify a constant stressor level at which a resistance element goes extinct over multiple serial passages. For an antibiotic resistance element, this would be a sub-MIC level of antibiotic that impedes growth, but does not impose a large enough growth defect to allow persistence of the element. With baseline stressor environment established, one can run high-throughput batch cultures, each receiving a randomized amount of antibiotic each passage, and with control wells receiving the same mean amount). Resistance could be measured as a population mean, as in Notley-McRobb et al. (11). The model predicts that the mean level of resistance in the noisy communities will exceed that in the constant-stressor controls. Even in the presence of additional mechanisms evolving over time, the impact of noise on overall resistance levels should still be observable through community-wide assays. The distribution of stress resistance levels observed in this experiment could also be compared to those found in nature (12).

Our theory has explored only one form of stressor fluctuations. In addition to interbatch stress level changes, stressor intensity may also change during the batch, e.g., antibiotics can be produced by other microbes, resulting in nontrivial stressor dynamics (for a chemostat analysis of these dynamics, see ref. 29). This may lead to large departures from our predicted behaviors: For example, such antisymmetric microbial interactions have been found in theory to lead to rock-paper-scissor dynamics (48). Furthermore, we have not considered the case where the dead bacteria contribute nutrient to the environment. Allowing such recycling may weaken the debtor advantage since instead of depriving the competitor of nutrient the debtor would then simply store and then release the nutrient. In summary, while this

manuscript covers the impact of exogenous stressors, to elucidate the impact of endogenous stressors on debt will require further work.

Focusing on the fundamental mechanisms underlying microbial debt, we considered only two species and a single nutrient. Yet, natural microbial communities typically feature many coexisting species. The mortality (ω, Ω) debt trade-off is not capable of supporting two species, so it would not support multiple species coexistence. Conversely, the affinity debt trade-off may support more than two species coexisting but may require fine-tuning (41). Investigating debt dynamics within complex, randomly assembled ecosystems (49) may shed light on the functioning of multispecies communities, such as the gut microbiome. Natural microbial communities also tend to feature more than the single resource assumed in our model. Previously, we demonstrated the "early-bird" effect, where the presence of multiple resources can amplify the benefit of an early growth advantage within a batch (24). This "early-bird" microbe can leverage its larger population size later in the batch to deplete resources it may not specialize in, depriving competitors. Thus, we expect debt dynamics to influence ecosystems with multiple species and resources in nontrivial ways.

Evolution is an important factor to consider, as the emergence of new variants of debtor and nondebtor occurs by mutation and subsequent competition with their ancestors. A promising direction to analyze the evolution of debt strategies is by using adaptive dynamics (50). Evolution may lead to the dominance of a single strain in the chemostat context, as it tends to minimize the steady-state nutrient level—the phenomenon of "pessimization" observed widely in adaptive dynamics (50). Pessimization is consistent with the pH 7 chemostat results of Notley-McRobb et al. (11), where the debtor dominates. At other pH values, partial *rpoS* mutants emerged and the chemostat did not reach steady state, so we cannot conclude whether the pessimization principle held in these cases. Note that later work from the same authors demonstrated that it is possible to qualitatively predict the outcomes of such evolution experiments using a chemostat theory (31). In a serial dilution context, it unclear whether the chemostat "pessimization" intuition holds, particularly as the switch from chemostat to serial dilution also can introduce additional stressors. For example, microbes can substantially acidify growth media, exposing the community to stress at the end of the batch (51). Such pH stress effectively increases the cost of debt beyond what is currently in our model. Additionally, close matching of these evolution data may require additional information on the shape of the debt trade-off surface (9, 31), outside the scope of this manuscript.

Through the ages, debt has been an ever-present part of human life (52). Yet the omnipresence of debt in human life mirrors a much older and more basic notion. When competition for resources is fierce and resource levels change with time, a "grow now, pay later" strategy can be exploited to gain an advantage over one's competitors, a manifestation of the "early-bird" effect (24). Such an early-bird strategy is built on depriving competitors of resources by growing quickly, even if it means paying a significant future cost. Our work has shed light on how such fundamental trade-offs influence the world.

Materials and Methods

This manuscript contains no new experimental data; hence, no experimental methods are detailed. For details of the mathematical derivations, data fitting, and analyses, see *SI Appendix*. Numerical simulations of the serial dilutions model were carried out in MATLAB on the Hebrew University's research computing cluster.

Data, Materials, and Software Availability. Simulation code and results data have been deposited in Github (https://github.com/AmirErez/MicrobialDebt) (53).

ACKNOWLEDGMENTS. This work was partially funded by AE's startup grant at the Hebrew University. We thank Nathalie Balaban, Po-Yi Ho, and Anthony Lyndon Shiver for critically reading this manuscript. J.G.L. was supported by a Stanford Baker Fellowship.

Author affiliations: [a]Department of Bioengineering, Stanford University, Stanford, CA 94305; [b]Racah Institute of Physics, The Hebrew University, Jerusalem 9190401, Israel; [c]Department of Applied Physics, Stanford University, Stanford, CA 94305; and [d]Institute for Theoretical Physics, Utrecht University, Utrecht 3584 CC, Netherlands

1. J. Lloyd-Price, G. Abu-Ali, C. Huttenhower, The healthy human microbiome. *Genome Med.* **8**, 51 (2016).
2. A. Crits-Christoph *et al.*, Colonization patterns of soil microbial communities in the Atacama Desert. *Microbiome* **1**, 28 (2013).
3. S. Lladó, R. López-Mondéjar, P. Baldrian, Forest soil bacteria: Diversity, involvement in ecosystem processes, and response to global change. *Microbiol. Mol. Biol. Rev.* **81**, e00063–16 (2017).
4. L. W. Kelly, A. F. Haas, C. E. Nelson, Ecosystem microbiology of coral reefs: Linking genomic, metabolomic, and biogeochemical dynamics from animal symbioses to reefscape processes. *mSystems* **3**, e00162–17 (2018).
5. F. Abram, T. Arcari, D. Guerreiro, C. P. O'Byrne, "Chapter four - evolutionary trade-offs between growth and survival: The delicate balance between reproductive success and longevity in bacteria" in Microbial Physiology, R. K. Poole, D. J. Kelly, Eds. (Academic Press, 2021), vol. 79, pp. 133–162.
6. M. Linkevicius, J. M. Anderssen, L. Sandegren, D. I. Andersson, Fitness of *Escherichia coli* mutants with reduced susceptibility to tigecycline. *J. Antimicrobial. Chemother.* **71**, 1307–1313 (2016).
7. V. Patel, N. Matange, Adaptation and compensation in a bacterial gene regulatory network evolving under antibiotic selection. *eLife* **10**, e70931 (2021).
8. A. H. Melnyk, A. Wong, R. Kassen, The fitness costs of antibiotic resistance mutations. *Evol. Appl.* **8**, 273–283 (2015).
9. K. Phan, T. Ferenci, The fitness costs and trade-off shapes associated with the exclusion of nine antibiotics by OmpF porin channels. *ISME J.* **11**, 1472–1482 (2017).
10. S. Nair *et al.*, Nutrient limitation magnifies fitness costs of antimalarial drug resistance mutations. *Antimicrobial. Agents Chemother.* **66**, e01529–21 (2022).
11. L. Notley-McRobb, T. King, T. Ferenci, rpoS mutations and loss of general stress resistance in *Escherichia coli* populations as a consequence of conflict between competing stress responses. *J. Bacteriol.* **184**, 806–811 (2002).
12. E. Y. Valencia, J. P. Barros, T. Ferenci, B. Spira, A broad continuum of *E. coli* traits in nature associated with the trade-off between self-preservation and nutritional competence. *Microbial. Ecol.*, 1–15 (2022).
13. N. Q. Balaban, J. Merrin, R. Chait, L. Kowalik, S. Leibler, Bacterial persistence as a phenotypic switch. *Science* **305**, 1622–1625 (2004).
14. E. Kussell, S. Leibler, Phenotypic diversity, population growth, and information in fluctuating environments. *Science* **309**, 2075–2078 (2005).
15. E. Kussell, R. Kishony, N. Q. Balaban, S. Leibler, Bacterial persistence: A model of survival in changing environments. *Genetics* **169**, 1807–1814 (2005).
16. O. Fridman, A. Goldberg, I. Ronin, N. Shoresh, N. Q. Balaban, Optimization of lag time underlies antibiotic tolerance in evolved bacterial populations. *Nature* **513**, 418–421 (2014).
17. S. A. Smits *et al.*, Seasonal cycling in the gut microbiome of the Hadza hunter-gatherers of Tanzania. *Science* **357**, 802–806 (2017).
18. J. F. Brooks *et al.*, The microbiota coordinates diurnal rhythms in innate immunity with the circadian clock. *Cell* **184**, 4154–4167.e12 (2021).
19. V. Diwan, C. S. Lundborg, A. J. Tamhankar, Seasonal and temporal variation in release of antibiotics in hospital wastewater: Estimation using continuous and grab sampling. *PLoS One* **8**, e68715 (2013).
20. I. Cvijović, B. H. Good, E. R. Jerison, M. M. Desai, Fate of a mutation in a fluctuating environment. *Proc. Natl. Acad. Sci. U.S.A.* **112**, E5021–E5028 (2015).
21. J. Monod, *Recherches sur la croissance des cultures bacteériennes* (Hermann and Cie, 1942).
22. J. E. Goldford *et al.*, Emergent simplicity in microbial community assembly. *Science* **361**, 469 (2018).
23. N. Meroz, N. Tovi, Y. Sorokin, J. Friedman, Community composition of microbial microcosms follows simple assembly rules at evolutionary timescales. *Nat. Commun.* **12**, 2891 (2021).
24. A. Erez, J. G. Lopez, B. G. Weiner, Y. Meir, N. S. Wingreen, Nutrient levels and trade-offs control diversity in a serial dilution ecosystem. *eLife* **9**, e57790 (2020).
25. A. Erez, J. G. Lopez, Y. Meir, N. S. Wingreen, Enzyme regulation and mutation in a model serial-dilution ecosystem. *Phys. Rev. E* **104**, 044412 (2021).
26. P. Y. Ho, B. H. Good, K. C. Huang, Competition for fluctuating resources reproduces statistics of species abundance over time across wide-ranging microbiotas. *eLife* **11**, e75168 (2022).
27. L. Pacciani-Mori, A. Giometto, S. Suweis, A. Maritan, Dynamic metabolic adaptation can promote species coexistence in competitive microbial communities. *PLOS Comput. Biol.* **16**, e1007896 (2020).

28. A. Aranda-Diaz *et al*., Assembly of gut-derived bacterial communities follows "early-bird" resource utilization dynamics. bioRxiv [Preprint] (2023). https://www.biorxiv.org/content/10.1101/2023.01.13.523996v1.full (Accessed 16 December 2023).
29. S. B. Hsu, P. Waltman, A survey of mathematical models of competition with an inhibitor. *Math. Biosci.* **187**, 53–91 (2004).
30. R. E. Lenski, S. E. Hattingh, Coexistence of two competitors on one resource and one inhibitor: A chemostat model based on bacteria and antibiotics. *J. Theor. Biol.* **122**, 83–93 (1986).
31. R. Maharjan *et al*., The form of a trade-off determines the response to competition. *Ecol. Lett.* **16**, 1267–1276 (2013).
32. A. D. Letten, A. R. Hall, J. M. Levine, Using ecological coexistence theory to understand antibiotic resistance and microbial competition. *Nat. Ecol. Evol.* **5**, 431–441 (2021).
33. P. Chesson, Multispecies competition in variable environments. *Theor. Popul. Biol.* **45**, 227–276 (1994).
34. M. Basan *et al*., A universal trade-off between growth and lag in fluctuating environments. *Nature* **584**, 470–474 (2020).
35. J. Lin, M. Manhart, A. Amir, Evolution of microbial growth traits under serial dilution. *Genetics* **215**, 767–777 (2020).
36. K. Phan, T. Ferenci, A design-constraint trade-off underpins the diversity in ecologically important traits in species *Escherichia coli*. *ISME J.* **7**, 2034–2043 (2013).
37. Y. Kaplan *et al*., Observation of universal ageing dynamics in antibiotic persistence. *Nature* **600**, 290–294 (2021).
38. A. Posfai, T. Taillefumier, N. S. Wingreen, Metabolic trade-offs promote diversity in a model ecosystem. *Phys. Rev. Lett.* **118**, 028103 (2017).
39. C. Tarayre *et al*., Characterisation of phosphate accumulating organisms and techniques for polyphosphate detection: A review. *Sensors* **16**, 797 (2016).
40. T. Song *et al*., Fitness costs of rifampicin resistance in mycobacterium tuberculosis are amplified under conditions of nutrient starvation and compensated by mutation in the β subunit of RNA polymerase. *Mol. Microbiol.* **91**, 1106–1119 (2014).
41. Y. Fridman, Z. Wang, S. Maslov, A. Goyal, Fine-scale diversity of microbial communities due to satellite niches in boom and bust environments. *PLOS Comput. Biol.* **18**, e1010244 (2022).
42. J. Rivera-Pinto *et al*., A new perspective for microbiome analysis. *mSystems* **3**, e00053–18 (2018).
43. J. Aitchison, The statistical analysis of compositional data. *J. R. Stat. Soc.: Ser. B (Methodol.)* **44**, 139–160 (1982).
44. J. Friedman, E. J. Alm, Inferring correlation networks from genomic survey data. *PLOS Comput. Biol.* **8**, e1002687 (2012).
45. R. A. Sorg *et al*., Collective resistance in microbial communities by intracellular antibiotic deactivation. *PLoS Biol.* **14**, e2000631 (2016).
46. E. M. Brown, D. Nathwani, Antibiotic cycling or rotation: A systematic review of the evidence of efficacy. *J. Antimicrobial. Chemother.* **55**, 6–9 (2005).
47. G. F. Webb, E. M. D'Agata, P. Magal, S. Ruan, A model of antibiotic-resistant bacterial epidemics in hospitals. *Proc. Natl. Acad. Sci. U.S.A.* **102**, 13343–13348 (2005).
48. E. D. Kelsic, J. Zhao, K. Vetsigian, R. Kishony, Counteraction of antibiotic production and degradation stabilizes microbial communities. *Nature* **521**, 516–519 (2015).
49. R. Marsland III *et al*., Available energy fluxes drive a transition in the diversity, stability, and functional structure of microbial communities. *PLoS Comput. Biol.* **15**, e1006793 (2019).
50. O. Diekmann, A beginner's guide to adaptive dynamics. *Banach Center Publ.* **63**, 47–86 (2002).
51. C. Ratzke, J. Denk, J. Gore, Ecological suicide in microbes. *Nat. Ecol. Evol.* **2**, 867–872 (2018).
52. D. Graeber, *Debt: The First 5,000 Years* (Melville House, Brooklyn, NY, 2012). Reprint edition.
53. A. Erez, J. G. Lopez, Microbial Debt. GitHub. https://github.com/AmirErez/MicrobialDebt. Deposited 26 July 2023.